



# Chemometric assessment and investigation of mechanism involved in photo-Fenton and TiO<sub>2</sub> photocatalytic degradation of the artificial sweetener sucralose in aqueous media

P. Calza<sup>a</sup>, V.A. Sakkas<sup>b,\*</sup>, C. Medana<sup>c</sup>, A.D. Vlachou<sup>b</sup>, F. Dal Bello<sup>c</sup>, T.A. Albanis<sup>b</sup>

<sup>a</sup> Department of Chemistry and NIS Centre, University of Torino, via P. Giuria 7, 10125 Torino, Italy

<sup>b</sup> Department of Chemistry, University of Ioannina, Ioannina 45110, Greece

<sup>c</sup> Department of Chemistry, University of Torino, via P. Giuria 5, 10125 Torino, Italy

## ARTICLE INFO

### Article history:

Received 7 June 2012

Received in revised form 1 August 2012

Accepted 29 August 2012

Available online 10 September 2012

### Keywords:

Photocatalysis

Photo-Fenton

TiO<sub>2</sub>

Experimental design

Sucralose

## ABSTRACT

Chemometric optimization tools were employed, such as experimental design and response surface methodology (RSM) to assess the efficiency of two advanced oxidation processes (AOPs): homogeneous Fenton (Fe<sup>II</sup>/H<sub>2</sub>O<sub>2</sub>) and heterogeneous (TiO<sub>2</sub>) photocatalysis for the degradation of the artificial sweetener sucralose. The aqueous samples were irradiated under a variety of experimental conditions (pH, light intensity) and with different amounts of H<sub>2</sub>O<sub>2</sub>, Fe(II), TiO<sub>2</sub>. The use of RSM allowed fitting the optimal values of the parameters leading to the degradation of the contaminant. Also, a single polynomial expression modeling the reaction was obtained for both AOPs.

The intermediates formed during the photocatalytic and photo-Fenton process were investigated and characterized by means of HPLC/HRMS. The photocatalysed transformation of sucralose proceeds through the formation of few (eight) products, involving four different pathways: hydroxylation of the molecule, oxidation of the alcohol function, dechlorination and the cleavage of glycoside bond. All the identified intermediates were easily degraded and within four hours of irradiation complete mineralization was achieved. A comparison with Photo-Fenton reaction was also reported.

In addition Microtox bioassay (*Vibrio fischeri*) was employed in evaluating the ecotoxicity of solutions treated by heterogeneous photocatalysis. Results clearly demonstrate the efficiency of the photocatalytic process in the detoxification of the irradiated solutions.

© 2012 Elsevier B.V. All rights reserved.

## 1. Introduction

Sucralose (also known as Splenda or SucraPlus) (1,6-dichloro-1,6-dideoxy-β-D-fructofuranosyl-4-chloro-4-deoxy-R-galactopiranoside) is a new artificial sweetener synthesized by chlorinating sucrose. It is widely used in more than 80 countries, mostly in the USA, where an average concentration of 17.6 μg/L was found in wastewaters [1]. Screening on European rivers has shown concentrations up to 1 μg/L, especially in the United Kingdom, Belgium, France, Italy, Netherlands, Switzerland, Spain, Norway and Sweden [2].

Sucralose is scarcely absorbed and almost 85% is excreted [3], however, assesses potential adverse effects on health, since it provokes symptoms, such as, increase in blindness, mineralization of pelvic area and epithelial hyperplasia [4,5]. Combination of toxicological risk and environmental persistence suggests a possible

environmental hazard of this molecule, although acute effects would be rather unlikely at the concentration levels present in the environment.

Sucralose exhibits a high stability and persistence with a half-life of several years [6]. Hydrolysis accomplished at high temperatures and low pH highlighted the cleavage of glycoside bond with the formation of 1,6-dichloro-1,6-dideoxy-D-fructose and 4-chloro-4-deoxy-D-galactose [7,8]. The octanol–water partition coefficient (log K<sub>ow</sub>) of sucralose is 0.3 [9], that allows to foresee a greater presence in the aqueous phase and a limited bioaccumulation [10]. Sucralose is considered as an emerging contaminant due to its occurrence in environmental waters and persistence.

Little is known about the fate and environmental behavior of sucralose (partitioning, transport, degradation, interaction with other environmental media) after use. In this sense, the present study aims to comprehend the environmental transformations followed by this substance. Simulated solar irradiation using photo-Fenton and titania suspensions as catalysts are employed to assess the decomposition of sucralose, to identify intermediates, as well as to elucidate mechanistic details of the degradation under both

\* Corresponding author. Tel.: +30 26510 08303; fax: +30 26510 08795.

E-mail address: [vsakkas@cc.uoi.gr](mailto:vsakkas@cc.uoi.gr) (V.A. Sakkas).

processes. According to our knowledge this is the first time that the photocatalyzed transformation of sucralose is examined. The study assesses the degradation of sucralose under different aspects. For the optimization of the degradation processes, a statistical model based on multivariate analysis has been developed to study the simultaneous effect of Fe(II)/H<sub>2</sub>O<sub>2</sub>/pH and TiO<sub>2</sub>/light intensity, respectively, for homogeneous photo-Fenton and heterogeneous titania photocatalytic treatments. Another aspect of this work was the identification of possible intermediates as well as the determination of the total mineralization during the process. For this reason, powerful analytical techniques such as liquid chromatography coupled to mass-spectrometry (LC–MS) were employed. In addition the toxicity of water resulting from the photocatalytic process was evaluated by using Microtox bioassay (*Vibrio fischeri*).

## 2. Experimental

### 2.1. Materials and reagents

Sucralose (purity 98%), sodium hydrogen carbonate and potassium carbonate were all purchased by Sigma–Aldrich, acetonitrile (Supergradient HPLC grade) was obtained by Scharlau and sodium chloride (99.5%) was provided from Carlo Erba. FeSO<sub>4</sub>·7H<sub>2</sub>O and H<sub>2</sub>O<sub>2</sub> (30%, w/v) used as reagents were obtained by Merck (Darmstadt, Germany). The Fenton reaction was terminated at regular time intervals by adding anhydrous Na<sub>2</sub>SO<sub>3</sub> (Sigma–Aldrich). TiO<sub>2</sub> was Degussa P25 (surface area ~50 m<sup>2</sup>/g with a particle size of ~25 nm), supplied by Degussa AG (anatase:rutile 75:25). The water used for the preparation of solutions and eluents was obtained by a MilliQ system. The pH of the aqueous media was adjusted by adding the required amount of 1 M H<sub>2</sub>SO<sub>4</sub> (Merck) aqueous solution. All reagents employed were not subjected to any further purification.

### 2.2. Experimental set-up and irradiation procedures

Irradiation experiments of sucralose were carried out on stirred aqueous solutions contained in Pyrex glass cells. Degradation was performed on 5 mL volume of aqueous sucralose solutions or suspensions under a variety of experimental conditions (pH/H<sub>2</sub>O<sub>2</sub>/Fe<sup>II</sup> – for photo-Fenton, and TiO<sub>2</sub>, light intensity – for heterogeneous photocatalysis), according to the experimental design (Tables 1 and 2). Irradiation was carried out using a Suntest CPS+ apparatus from Heraeus (Hanau, Germany) equipped with a Xenon arc lamp (1500 W) and glass filters restricting the transmission of wavelengths below 290 nm. The device comes with internal module that can adjust the light intensity from 25 to 750 W/m<sup>2</sup>. The corresponding light dose for 10 min of irradiation was 450 kJ/m<sup>2</sup>. Chamber and black panel temperature were regulated by pressurized air-cooling circuit and monitored using thermocouples supplied by the manufacturer.

For identification of intermediates Pyrex glass cells were filled with 5 mL of sucralose (15 mg/L) and TiO<sub>2</sub> (200 mg/L). Illumination was provided with a Philips TLK/05 40 W lamp, with emission maximum at 360 nm. The temperature reached during irradiation was 38 ± 2 °C. In all cases, to remove TiO<sub>2</sub> particles the solution samples were passed through 0.45 μm filters and were further analyzed with the appropriate analytical technique.

50 mL of more concentrated sucralose samples (200 mg/L) were subjected to 5 and 10 min of irradiation with TiO<sub>2</sub> and then were concentrated to 1 mL in a Bruker lyophilizer; MS<sup>2</sup> spectra were collected by HPLC/MS.

### 2.3. Analytical techniques

#### 2.3.1. HPLC-MS

Analyses were performed by ESI source, both in positive and negative ionization mode. The negative ion mode generates a signal 2–3 orders of magnitude weaker than positive-mode signal; for this reason only data performed in positive ion mode are shown. For sucralose, LOD and LOQ were 30 and 100 μg/L, respectively.

The chromatographic separations followed by MS analysis were run on a C<sub>18</sub> column Phenomenex Luna, 150 mm × 2.0 mm, thermostated at 30 °C using an Ultimate 3000 HPLC instrument (Dionex, Milan, Italy). Injection volume was 20 μL and flow rate 200 μL/min. Gradient mobile phase composition was adopted: 5/95 to 100/0 in 35 min. acetonitrile/formic acid 0.05% in water. ALTO Orbitrap mass spectrometer (Thermo Scientific, Bremen, Germany) equipped with an atmospheric pressure ESI interface was used as detector. The LC column effluent was delivered into the ion source using nitrogen as sheath and auxiliary gas. The source voltage was set at 4.5 kV. The heated capillary temperature was maintained at 265 °C. The acquisition method used was previously optimized in the tuning sections for the parent compound (capillary, magnetic lenses and collimating octapoles voltages) to achieve maximum sensitivity. The tuning parameters adopted for the ESI source have been the following: capillary voltage 7.00 V, tube lens 55 V; for ions optics, multipole 00 offset – 1.50 V, lens 0 voltage – 5.50 V, multipole 0 offset – 4.75 V, lens 1 voltage – 36.00 V, gate lens voltage – 80.00 V, multipole 1 offset – 19.50 V, front lens voltage – 5.50 V. Mass accuracy of recorded ions (vs calculated) was ± 5 millimass units (mmu) (without internal calibration).

#### 2.3.2. Ion chromatography

An ion chromatograph equipped with a Dionex 40 gradient pump, LC 30 chromatograph enclosure and a Dionex ED 40 conductimetric detector was employed. The anions were analyzed using a Dionex AS9HC anion-exchange column equipped with a guard column Dionex IonPac AG9-HC, 10 mM NaHCO<sub>3</sub> and 4 mM K<sub>2</sub>CO<sub>3</sub> as eluent and a flow rate of 0.9 mL/min. In these experimental conditions, the retention time for chloride was 7.33 min.

#### 2.3.3. Measurement of total organic carbon

Total organic carbon (TOC) was measured using a Shimadzu TOC-5000 analyzer which is based on sample oxidation on platinum catalyst at a temperature of 680 °C. The instrument calibration was performed with the analysis of samples of potassium hydrogen phthalate.

#### 2.3.4. Toxicity measurements

The toxicity of sucralose solutions and of aqueous samples collected at different irradiation times, was examined by Microtox Model 500 Toxicity Analyzer. Toxicity was evaluated by monitoring changes in the natural emission of the luminescent bacteria *V. fischeri* when exposed to toxic compounds. Freeze-dried bacteria, reconstitution solution, diluent (2% NaCl) and an adjustment solution (non-toxic 22% sodium chloride) were obtained from Azur. Briefly, samples in five dilutions were tested in a medium containing 2% sodium chloride, and luminescence was recorded after 5 and 15 min of incubation at 15 °C. The inhibition of the luminescence, compared with a toxic-free control to give the percentage of inhibition, was calculated following the established protocol of the Microtox calculation program.

### 2.4. Experimental design

Preliminary investigations (Plackett–Burman screening design) were carried out to select the most suitable parameters that affect

**Table 1**  
Central composite experimental design and results for photo-Fenton photocatalysis of sucralose.

Fe (mg/L) ( $x_1$ )	H <sub>2</sub> O <sub>2</sub> (mmol L <sup>-1</sup> ) ( $x_2$ )	pH ( $x_3$ )	Degradation % (experimental)	Degradation % (predicted)
1 (-1)	1.357 (-1)	2.5 (-1)	62.7	62.7
5 (+1)	1.357 (-1)	2.5 (-1)	74.1	74.9
1 (-1)	4.071 (+1)	2.5 (-1)	64.4	65.0
5 (+1)	4.071 (+1)	2.5 (-1)	79.1	80.1
1 (-1)	1.357 (-1)	3.5 (+1)	68.8	68.9
5 (+1)	1.357 (-1)	3.5 (+1)	78.4	78.9
1 (-1)	4.071 (+1)	3.5 (+1)	66.5	66.8
5 (+1)	4.071 (+1)	3.5 (+1)	78.6	79.6
3 (0)	2.714 (0)	3 (0)	90.4	90.9
3 (0)	2.714 (0)	3 (0)	91.2	90.9
3 (0)	2.714 (0)	3 (0)	90.8	90.9
0.36 (-1.68)	2.714 (0)	3 (0)	74.8	74.7
6.36 (+1.68)	2.714 (0)	3 (0)	97.1	95.7
3 (0)	0.434 (-1.68)	3 (0)	67.1	66.8
3 (0)	4.994 (+1.68)	3 (0)	70.5	69.3
3 (0)	2.714 (0)	2 (-1.68)	64.9	64.0
3 (0)	2.714 (0)	4 (+1.68)	69.4	68.8

significantly (confidence level 95%) the homogeneous (photo-Fenton) and heterogeneous (TiO<sub>2</sub>) photocatalytic efficiency of sucralose in aqueous media. It was observed that initial concentrations of Fe(II), H<sub>2</sub>O<sub>2</sub>, and pH for the photo-Fenton system, as well as light intensity and titania amount for the photo TiO<sub>2</sub> were the most important parameters. Therefore, they were subjected to further investigation with the employment of chemometric tools and response surface methodology (RSM). The central composite design (CCD) was employed to analyze the simultaneous effect of H<sub>2</sub>O<sub>2</sub>, Fe(II) and pH (photo-Fenton) as well as light intensity and TiO<sub>2</sub> concentration in the photocatalytic degradation process, and to evaluate the interactions between the studied variables. The central composite design considered low (-1) and high (+1) levels, as well as central points (0) for the the studied variables, respectively. The experimental conditions for all runs and the results (response factor (Y)-corresponding to sucralose degradation % after 15 min of irradiation) obtained are summarized in Tables 1 and 2. Statistica 7.0 (StatSoft, Inc. Tulsa, USA) statistical package was used to generate the experimental matrix.

### 3. Results and discussion

#### 3.1. Sucralose stability, photolysis and kinetics

Experiments were carried out before the development of the experimental design, to evaluate the extent of adsorption, hydrolysis and photolysis processes on the transformation. Results obtained, showed, that the experiments occurred in a pure photocatalytic regime, where hydrolysis and direct photolysis processes can be neglected. Moreover, in the considered times, no degradation occurs in the dark (less than 3% of conversion) when Fe<sup>II</sup>/H<sub>2</sub>O<sub>2</sub> (Fenton reagent) are initially added to aqueous solutions. Sucralose

degradation was observed by irradiation of Fenton (photo-Fenton reaction), due to the formation of additional hydroxyl radicals but also to recycling of ferrous catalyst by reduction of Fe<sup>III</sup>. In this way, the concentration of Fe<sup>II</sup> is increased and the overall reaction is accelerated. This process, as well as TiO<sub>2</sub> and was further assessed by experimental design and RSM. Several experimental results indicated that the destruction rates of photocatalytic oxidation of various organic contaminants over illuminated TiO<sub>2</sub> followed a saturated trend with increasing the substrate concentration similar to a Langmuir–Hinshelwood behaviour that was strongly criticized [11,12]. These studies have shown that adsorption/desorption equilibrium is not established under irradiation and in catalysis achievements, such an equilibrium is a major requirement for the validity of the L–H model. Taking into consideration the recent point of discussion with regard to kinetics interpretation in photocatalytic reactions [13], to reduce experiments and related times for the development of multivariate approach, the efficiency of the photocatalytic procedures was evaluated as the degradation percentage after 15 min of light irradiation. This time period was chosen because distinguishable amounts of sucralose were obtained that allowed better comparison of the results.

#### 3.2. DoE–RSM optimization

Model validation is ensured by the most powerful numerical method, the employment of analysis of variance (ANOVA). A *P*-value less than 0.05 in the ANOVA table indicates the statistical significance of an effect at 95% confidence level. Positive sign indicates that the increase of the value of a variable will have as a consequence the increase of the efficiency of the photocatalytic method.

**Table 2**  
Central composite experimental design and results for TiO<sub>2</sub> photocatalysis of sucralose.

TiO <sub>2</sub> (mg/L) ( $x_1$ )	Light intensity (W/m <sup>2</sup> ) ( $x_2$ )	Degradation % (experimental)	Degradation % (predicted)
100 (-1)	520 (-1)	62.1	62.2
100 (-1)	680 (1)	73.9	74.7
300 (1)	520 (-1)	74.2	73.3
300 (1)	680 (1)	88.9	88.7
58.6 (-1.4142)	600 (0)	64.4	63.7
341.4 (1.4142)	600 (0)	80.6	81.4
200 (0)	486.88 (-1.4142)	66.43	67.0
200 (0)	713.12 (1.4142)	87.2	86.8
200 (0)	600 (0)	80.5	80.8
200 (0)	600 (0)	81.1	80.8
200 (0)	600 (0)	80.8	80.8

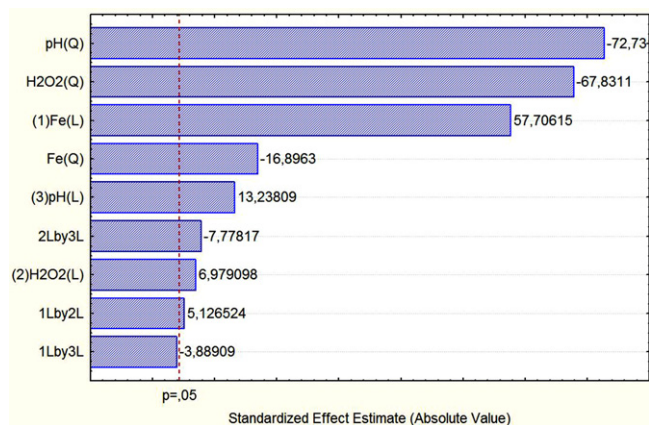


**Fig. 1.** Pareto Chart of standardized effects of the main effects for sucralose degradation%. The vertical dashed line indicated the level of significance at  $P=0.05$ .

Experimental results for both treatments (photo-Fenton and photo-TiO<sub>2</sub>) were fitted, by least-squares linear regression, to a polynomial quadratic equation as follows:

$$Y = b_0 + \sum_{i=1}^n b_i x_i + \sum_{i=1}^n \sum_{j=1}^n b_{ij} x_i x_j$$

where  $X_i$  were the studied factors for each treatment and the response  $Y$  was the degradation efficiency of sucralose (expressed as %) for photo-Fenton and TiO<sub>2</sub> process, respectively.

Moreover, Lack of Fit, which measures the failure of the model to represent data in the experimental domain at points which are not included in the regression [14], was also checked for both AOPs and was shown to be not significant relative to the pure error, indicating good response to the model. The model regression coefficients ( $R^2$ ) of 0.9955 and 0.9957 are in reasonable agreement with the experimental results of photo-Fenton and TiO<sub>2</sub> photocatalytic process, respectively, while the adjusted determination coefficients are also very high advocating for a high significance of the models. These data ensured a satisfactory correlation between the experimental and predicted values for both treatments.

### 3.2.1. Photo-Fenton treatment

The main effects, interaction effects as well as quadratic effects were evaluated through analysis of variance (ANOVA).  $P$ -values that were generated using STATISTICA 7.0 were used to identify the significance of each variable on the photocatalytic efficiency of sucralose degradation %. The results of statistical analysis showed that the quadratic terms pH ( $P=0.00019$ ), H<sub>2</sub>O<sub>2</sub> ( $P=0.00022$ ), Fe(II) ( $P=0.00348$ ), as well as all linear terms (pH:  $P=0.00567$  H<sub>2</sub>O<sub>2</sub>:  $P=0.01992$  Fe(II):  $P=0.00030$ ) were significant ( $P<0.05$ ). With regard to the interaction effects, the results have shown that changes between pH H<sub>2</sub>O<sub>2</sub> ( $P=0.01613$ ) and Fe(II) H<sub>2</sub>O<sub>2</sub> ( $P=0.03600$ ) have a significant effect on the photocatalytic performance of the photo-Fenton process (Fig. 1). Data analysis using the STATISTICA software at 95% confidence level yielded the following semi-empirical expression (Eq. (1)) in terms of significant coded factors:

$$Y_{\text{photo-Fenton}} = 90.88 + 6.24x_1 + 0.75x_2 + 1.43x_3 - 2.01x_1^2 - 8.09x_2^2 - 8.67x_3^2 + 0.72x_1x_2 - 1.1x_2x_3 \quad (1)$$

where  $x_1$ ,  $x_2$  and  $x_3$  are Fe(II), H<sub>2</sub>O<sub>2</sub>, and pH, respectively, while response  $Y_{\text{photo-Fenton}}$  is the efficiency of sucralose % removal, after a treatment time of 15 min.

Degradation efficiency is increased with increasing amounts of Fe(II), pH and H<sub>2</sub>O<sub>2</sub>, respectively, as can be inferred by the positive

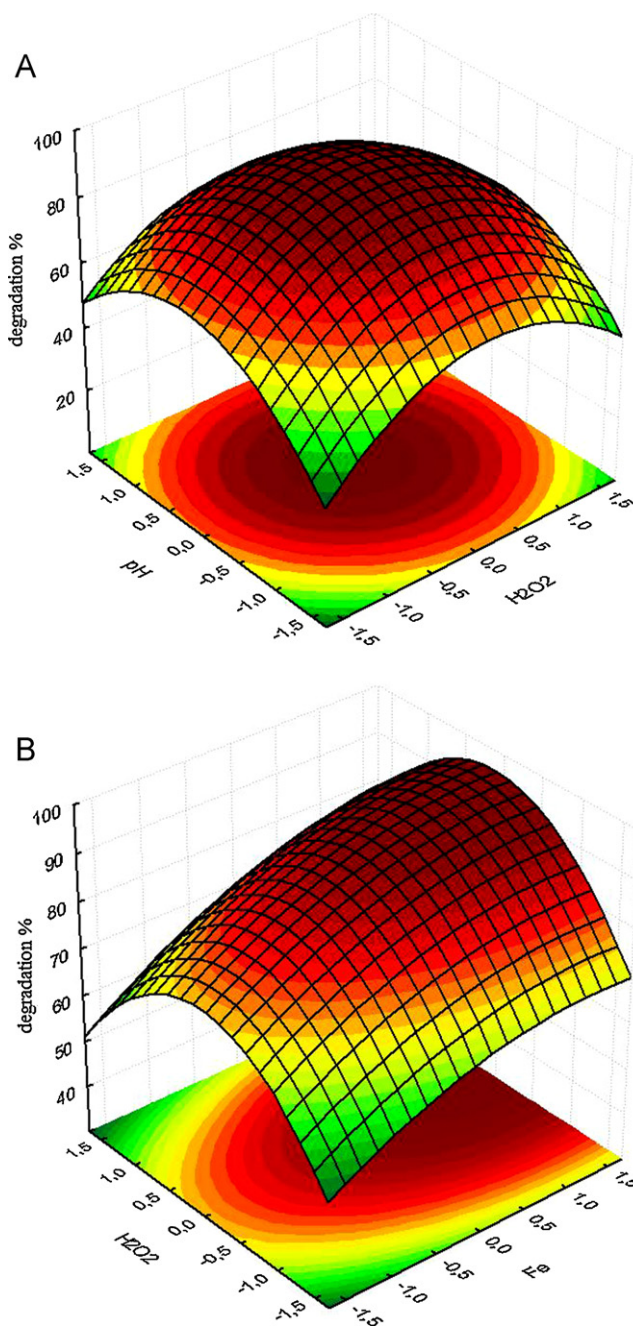


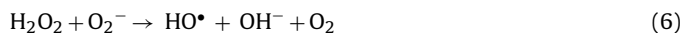
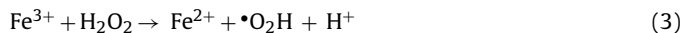
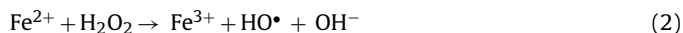
**Fig. 2.** Response surface showing the effect of (a) H<sub>2</sub>O<sub>2</sub> concentration and pH and (b) H<sub>2</sub>O<sub>2</sub> and Fe(II) concentration, on the degradation efficiency expressed as sucralose degradation% after 15 min irradiation. On axis of H<sub>2</sub>O<sub>2</sub>, value of 0.0 correspond to concentration of 2.714 mM, on pH, axis 0 value correspond to pH 3 and on Fe(II), axis value 0 correspond to 3 mg/L, as described in Table 1.

linear coefficients (Eq. (1)). However, an opposing driving tendency is observed when high values of the above variables were adopted, according to the negative quadratic coefficients.

With regard to the interaction effects between the investigated variables, the three-dimensional profiles of multiple non-linear regression models are depicted in Fig. 2. The shape of the response surface curves depicts the interactions between the studied factors  $x_2 \cdot x_3$  (pH/H<sub>2</sub>O<sub>2</sub>) and  $x_1 \cdot x_2$  (Fe<sup>II</sup>/H<sub>2</sub>O<sub>2</sub>), respectively.

The results indicate that sucralose conversion was increased by increasing the concentration of peroxide up to 2.714 mg/L (coded value 0, Fig. 2a). The degradation of sucralose is favored due to the

additionally hydroxyl radicals produced during the photo-Fenton process:



However, when high concentrations of  $\text{H}_2\text{O}_2$  are used, a decrease on the degradation yield was observed, due to reaction of  $\text{HO}^\bullet$  with  $\text{H}_2\text{O}_2$ , contributing to the  $\text{HO}^\bullet$  scavenging capacity [15]:



The photo-Fenton reaction is also strongly affected by the solution pH. The highest photocatalytic efficiency was observed at  $\text{pH} \approx 3$  (coded value 0). Generally, the optimal pH of the photo-Fenton reaction is around 3 [16] because the main species at pH 2–3,  $\text{Fe}(\text{OH})^{2+}(\text{H}_2\text{O})_5$ , is the one with the largest light absorption coefficient and quantum yield for  $\text{HO}^\bullet$  radical production, along with Fe(II) regeneration, in the range 280–370 nm. At  $\text{pH} > 3$  the possible formation of ferryl ion intermediate ( $\text{FeO}_2^+$ ) could be the cause of inhibition of sucralose degradation, producing a possible side reaction that interferes with the formation of hydroxyl radicals that are critical for the oxidation of the contaminant.

With respect to Fe(II) and  $\text{H}_2\text{O}_2$  interaction (at fixed  $\text{pH} = 3$ ) (Fig. 2b), increasing iron concentrations favored the treatment of sucralose especially at moderate amounts of  $\text{H}_2\text{O}_2$ . The negative quadratic effect of iron calculated from ANOVA may be explained by the fact that an excess of divalent iron ions provokes UV photon attenuation (penetrating into the reactive medium layer [17]). Photo-Fenton degradation efficiency inhibition, may be also attributed to the scavenging of hydroxyl radicals by ferrous ions (the reaction is faster than that of Eq. (7)).

According to the statistical analysis results for the optimum photo-Fenton reactor conditions, the best photocatalytic efficiency (96%) was attained operating at  $2.9 \text{ mmol L}^{-1}$  of  $\text{H}_2\text{O}_2$ ,  $6 \text{ mg/L}$  of Fe(II) and  $\text{pH} 3$ .

### 3.2.2. $\text{TiO}_2$ treatment

The performance of the  $\text{TiO}_2$  photocatalytic degradation of sucralose was also modeled. The predicted second-degree model for degradation % is represented in terms of coded values:

$$Y_{\text{TiO}_2} = 80.80 + 6.98x_1 + 6.25x_2 - 1.96x_1^2 - 4.12x_2^2 - 0.75x_1x_2 \quad (10)$$

At the experimental domain studied, light intensity and  $\text{TiO}_2$  displayed the strongest effects individually, with regard to the photocatalytic degradation of the target compound. Increase on the  $\text{TiO}_2$  photocatalytic performance was observed with increasing light intensity and  $\text{TiO}_2$  amount, respectively (positive linear coefficients). However, a decrease on the efficiency was observed at high values of the respective variables (negative quadratic coefficients). Although availability of active sites increases with catalyst loading, above the optimum value the increased turbidity of the suspension reduces the transmission of irradiation [18]. Results have also shown that interaction of the two variables is significant (confidence level 95%) and a 3-D representation between them is depicted in Fig. 3.

Irrespective of titania loading, an increase of the light intensity increases the degradation of the contaminant. Moreover, the profile

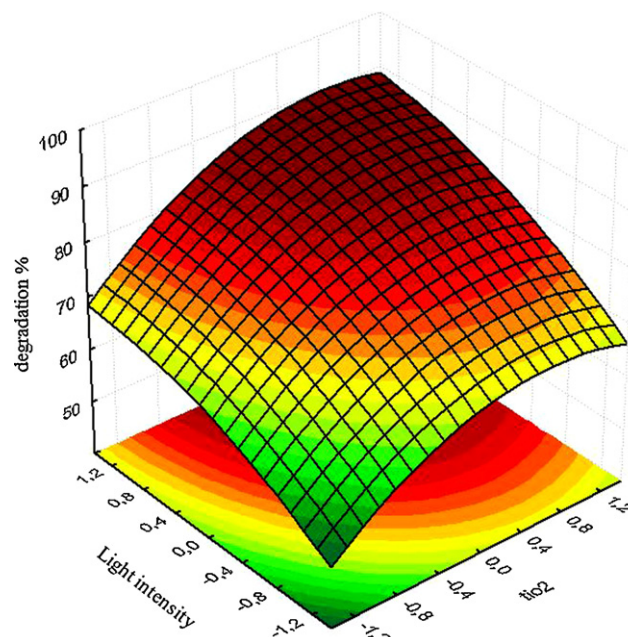


Fig. 3. Response surface showing the effect of  $\text{TiO}_2$  concentration and light intensity on the degradation rate expressed as sucralose degradation% after 15 min irradiation. On axis of  $\text{TiO}_2$ , value of 0.0 correspond to concentration of  $200 \text{ mg/L}$ , on light intensity, axis 0 value correspond to  $600 \text{ W/m}^2$ , as described in Table 2.

can be divided in two parts: in the beginning the degradation reaction seems to be proportional to the light intensity, thus confirming the photoinduced nature of the activation of the catalytic process, with the participation of photo-induced electrical charges (electrons and holes) to the reaction mechanism [19]. In other words, the incident photons are efficiently converted into active species that act in the degradation of the target compound. However, at higher values a decline on the photocatalytic rate was observed. Recombination of photoinduced  $e^-/h^+$  pairs occurs in some degree and it has been believed that this reduces quantum efficiency and the overall photocatalytic reaction rate [20,21]. Similar observations have been reported in the literature for other model compounds [22–24].

The highest photocatalytic efficiency (89%) of the photo- $\text{TiO}_2$  treatment was calculated at operating conditions of  $294 \text{ mg/L}$  of  $\text{TiO}_2$ , and  $698 \text{ W/m}^2$  light intensity.

A usual requirement of an efficient catalytic reaction is its application, or in other words the ability of the optimized method to provide accurate and precise results despite variations in equipment and conditions. For this reason the target compound was tested at the optimal conditions found from RSM, in natural river water ( $\text{pH} 7.9$ , conductivity  $295 \text{ mS/cm}$ , total dissolved solids  $188 \text{ mg/L}$ , total organic carbon  $2.693 \text{ mg/L}$ ). Results have shown that the response of interest (degradation efficiency) for both processes was not significantly influenced by changing the aqueous matrix from distilled to natural river water, demonstrating a degradation yield of 90% and 91% for photo-Fenton and  $\text{TiO}_2$ , respectively, after 15 min of illumination. These minor variations may be attributed to the presence of organic matter, as well as, reactive moieties and species such as  $\text{Cl}^-$ ,  $\text{HCO}_3^-$ ,  $\text{CO}_3^{2-}$  that compete for hydroxyl radicals and/or photocatalyst surface sites.

### 3.3. Characterization of sucralose intermediates

The formation of TPs, produced along with sucralose degradation through photocatalytic and photo-Fenton processes, was evaluated via HPLC/HRMS. The identification of transformation

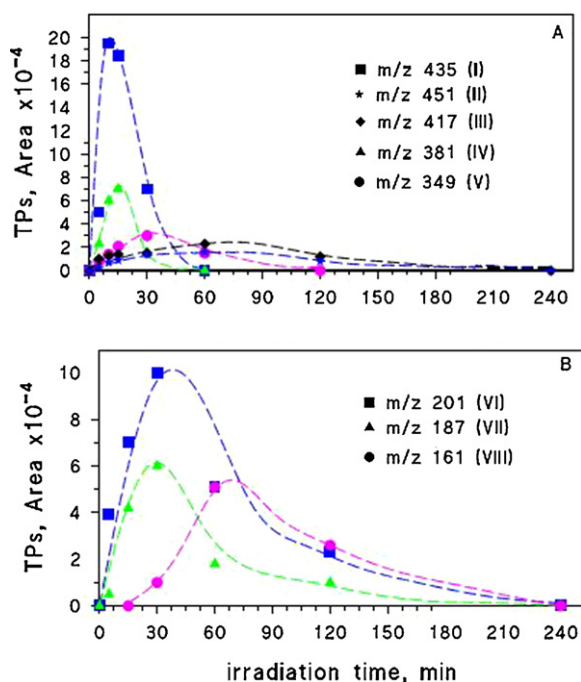


Fig. 4. Intermediates formed from sucralose degradation under illumination plotted as a function of the irradiation time in the presence of 200 mg/L TiO<sub>2</sub>.

products is a crucial task difficult to tackle, due to the lack of standards and scarce information available. In the present study, identification and structural elucidation of intermediates is based on the use of accurate mass measurements and fragmentation patterns. TPs evolution as a function of irradiation time was followed in both cases, but only TPs formed through TiO<sub>2</sub> photocatalytic process are plotted in Fig. 4.

First, a complete MS<sup>n</sup> study was performed on sucralose, to assess those that are the key product ions formed during sucralose breakdown and that will be considered in the structural attribution of unknown compounds. Table 3 collects all MS<sup>2</sup> and MS<sup>3</sup> product ions; all the formed ions could be linked together through the fragmentation pathways proposed (Scheme S1 of the Supporting Information).

The intense signal in positive mode can be attributed to [M+Na]<sup>+</sup>, and not to protonated molecule, as was already observed in previous studies [25]. MS<sup>2</sup> spectrum shows two key product ions at *m/z* 221.0094 and empirical formula C<sub>6</sub>H<sub>11</sub>O<sub>5</sub>ClNa attributed to glycoside moiety and at *m/z* 238.9749 and empirical formula C<sub>6</sub>H<sub>10</sub>O<sub>4</sub>Cl<sub>2</sub>Na, due to fructose moiety. A third product ion at *m/z* 203.0104 and empirical formula C<sub>6</sub>H<sub>9</sub>O<sub>4</sub>ClNa was formed and is well-matched with the glucoside moiety, also involving the loss of a water molecule from glycoside oxygen. The MS<sup>3</sup> spectrum shows loss of hydrochloric acid (*m/z* 167.0226), of water (*m/z* 149.0114) or of formic acid (*m/z* 137.0107), thus implying an easy detachment of the methylene moiety from the sugar ring.

### 3.3.1. Hydroxylation

Hydroxylated products were formed at detectable amounts only during TiO<sub>2</sub> treatment. A transformation product with *m/z* 434.9803 (labeled I) and empirical formula C<sub>12</sub>H<sub>19</sub>O<sub>9</sub>Cl<sub>3</sub>Na was attributed to monohydroxyl sucralose (+15.9939 Da). Looking closer to MS<sup>2</sup> spectrum, few key ions emerge (see Table 4). The formation of a product ion with *m/z* 237.0140 and empirical formula C<sub>6</sub>H<sub>11</sub>O<sub>6</sub>ClNa, is attributed to hydroxyl-glucose moiety and permits to allocate the hydroxyl group on the glucose moiety. We tentatively propose hydroxylation on 6-methyl position (see Fig. S1 and Scheme S2).

A TP with *m/z* 450.9608 (labeled II) and empirical formula C<sub>12</sub>H<sub>19</sub>O<sub>10</sub>Cl<sub>3</sub>Na was identified; it is consistent with the occurrence of a dihydroxylation on sucralose molecule (Table 4). MS<sup>2</sup> study did not permit to assign the positions for hydroxylation; however, we can assume that at least an hydroxyl function should be placed on chloromethyl moiety.

### 3.3.2. Oxidation

Few TPs were recognized as oxidized products, involving or not dechlorination. TP with *m/z* 416.9787 (labeled III) and empirical formula C<sub>12</sub>H<sub>17</sub>O<sub>8</sub>Cl<sub>3</sub>Na was formed through both photocatalytic and photo-Fenton processes; it produced a key ion at *m/z* 374.8679 in MS<sup>2</sup> spectrum, due to ketene loss and well-matched with oxidation of hydroxymethyl moiety to aldehyde function (see Table 4).

Two different TPs involving a partial (or complete) dechlorination were also identified during the photocatalytic process: TP at *m/z* 380.9958 (labeled IV), with empirical formula C<sub>12</sub>H<sub>16</sub>O<sub>8</sub>Cl<sub>2</sub>Na, and a TP at *m/z* 349.1686 (labeled V) and empirical formula C<sub>12</sub>H<sub>22</sub>O<sub>10</sub>Na.

Unfortunately it was not possible to accomplish a fragmentation study on these two TPs even on concentrated samples, due to their low signal-to-noise ratio. Thanks to the high resolution, however, we postulated a probable structure that is depicted in Scheme 1. TP IV will start an additional pathway involving dechlorination; TP V, whose formation involves complete dechlorination and monohydroxylation, reasonably derives from TP I.

### 3.3.3. Molecule breakage

Sucralose breakage occurs with both treatment processes and leads to the formation of two TPs that, on the basis on their empirical formula, should be attributed to the two portions of the sweetener, derived from glycoside or fructose moieties. The formation of a TP at *m/z* 200.9843 (labeled VI) and empirical formula C<sub>6</sub>H<sub>11</sub>O<sub>3</sub>Cl<sub>2</sub> was attributed to the fructose moiety. Differently from the previously described compounds, this TP is detected as [M+H]<sup>+</sup> instead of sodium adduct. TP at *m/z* 187.0095 (C<sub>6</sub>H<sub>9</sub>O<sub>3</sub>ClNa) (labeled VII) has been attributed to the other portion of the molecule; the presence of a single chlorine atom suggests that this TP is derived from the glycoside moiety through dehydration.

TP VI is subjected to dechlorination with the formation of another breakdown product at *m/z* 161.0401 (labeled VIII) (C<sub>5</sub>H<sub>11</sub>O<sub>2</sub>ClNa).

### 3.3.4. Sucralose transformation pathways

Based on the above characterized TPs and their evolution profiles, four different initial transformation pathways could be proposed for the photocatalytic process mediated by TiO<sub>2</sub> and are collected in Scheme 1. Conversely, sucralose transformation through photo-Fenton process proceeds only through two pathways, namely B and D, described below.

The first route, namely A, proceeds through hydroxylation of the molecule, involving monohydroxylation (I), followed by a further hydroxylation with formation of compound (II) or complete dechlorination with formation of TP V. The second way, namely B, accounts for oxidation of the alcohol function with the formation of TP III. A third route, namely C, involves dechlorination of the molecule; TP IV is formed through dechlorination. Pathway D, leads to the cleavage of glycoside bond with the formation of TP VI, formed through the detachment of fructose moiety and further transformed into the dechlorinated TP VII, and TP VIII, formed through detachment of glycoside moiety.

### 3.4. Mineralization

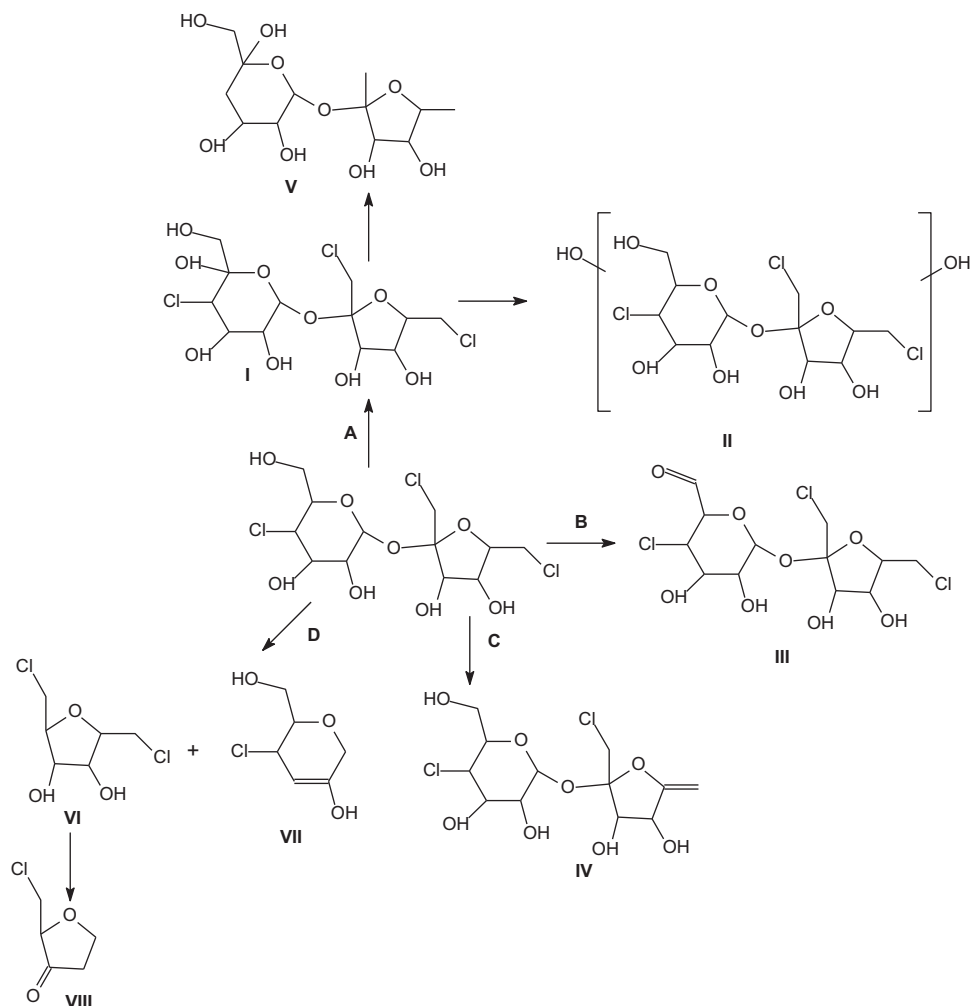
Sucralose and its intermediates were completely degraded, as arises from the temporal profiles shown in Figs. 4 and 5.

**Table 3**  
Main product ions formed from sucralose MS<sup>2</sup> and MS<sup>3</sup> spectra.

[M+Na] <sup>+</sup>	Δ mmu	t <sub>R</sub>	MS <sup>2</sup>	MS <sup>3</sup>
418.9864 C <sub>12</sub> H <sub>19</sub> Cl <sub>3</sub> O <sub>8</sub> Na	-9,166	14.04	221.0094 (100) (-C <sub>6</sub> H <sub>8</sub> O <sub>3</sub> Cl <sub>2</sub> ) 238.9749 (50) (-C <sub>6</sub> H <sub>9</sub> O <sub>4</sub> Cl) 203.0104 (40) (-C <sub>6</sub> H <sub>10</sub> O <sub>4</sub> Cl <sub>2</sub> )	203.0104 (100) (-H <sub>2</sub> O) 160.8994 (50) (-C <sub>2</sub> H <sub>4</sub> O <sub>2</sub> ) - 149.0114 (100) (-H <sub>2</sub> O, -HCl) 167.0226 (80) (-HCl) 137.0107 (40) (-CH <sub>2</sub> O, -HCl) 121.0157 (40) (-CH <sub>2</sub> O <sub>2</sub> , -HCl)

**Table 4**  
List of main [M+H]<sup>+</sup> and fragments coming from MS and MS<sup>n</sup> spectra obtained, together with their empirical formula and Δ mmu from sucralose intermediate compounds. In square bracket are quoted the relative ion abundances.

[M+Na] <sup>+</sup>	Label	t <sub>R</sub>	MS <sup>2</sup>
434.9803 C <sub>12</sub> H <sub>19</sub> O <sub>9</sub> Cl <sub>3</sub> Na	<b>I</b>	12.05	237.0140 (100) (-C <sub>6</sub> H <sub>8</sub> O <sub>3</sub> Cl <sub>2</sub> ) 219.0032 (40) (-C <sub>6</sub> H <sub>8</sub> O <sub>3</sub> Cl <sub>2</sub> , -H <sub>2</sub> O) 200.9893 (40) (-C <sub>6</sub> H <sub>8</sub> O <sub>3</sub> Cl <sub>2</sub> , -2H <sub>2</sub> O) 182.9787 (20) (-C <sub>6</sub> H <sub>8</sub> O <sub>3</sub> Cl <sub>2</sub> , -3H <sub>2</sub> O) 408.9502 (79) (-C <sub>2</sub> H <sub>2</sub> O) 374.8679 (36) (-C <sub>2</sub> H <sub>2</sub> O)
450.9608 C <sub>12</sub> H <sub>19</sub> O <sub>10</sub> Cl <sub>3</sub> Na	<b>II</b>	12.45	408.9502 (79) (-C <sub>2</sub> H <sub>2</sub> O)
416.9787 C <sub>12</sub> H <sub>17</sub> O <sub>8</sub> Cl <sub>3</sub> Na	<b>III</b>	13.30	374.8679 (36) (-C <sub>2</sub> H <sub>2</sub> O)
380.9958 C <sub>12</sub> H <sub>16</sub> O <sub>8</sub> Cl <sub>2</sub> Na	<b>IV</b>	13.47	-
349.1686 C <sub>12</sub> H <sub>22</sub> O <sub>10</sub> Na	<b>V</b>	12.30	-
200.9843 C <sub>6</sub> O <sub>3</sub> H <sub>11</sub> Cl <sub>2</sub>	<b>VI</b>	8.83	155.0127 (77) (-C <sub>2</sub> H <sub>6</sub> O, -CO) 96.9604 (10) (-CH <sub>3</sub> Cl, -HCl, -H <sub>2</sub> O) 84.9591 (12) (-CH <sub>3</sub> Cl, -CH <sub>3</sub> OCl)
187.0095 C <sub>6</sub> H <sub>9</sub> O <sub>3</sub> ClNa	<b>VII</b>	2.26	-
161.0401 C <sub>5</sub> H <sub>11</sub> O <sub>2</sub> ClNa	<b>VIII</b>	5.14	111.0149 (83) (-CH <sub>3</sub> Cl) 118.9856 (16) (-C <sub>2</sub> H <sub>2</sub> O)



**Scheme 1.** Initial transformation pathways involving sucralose.

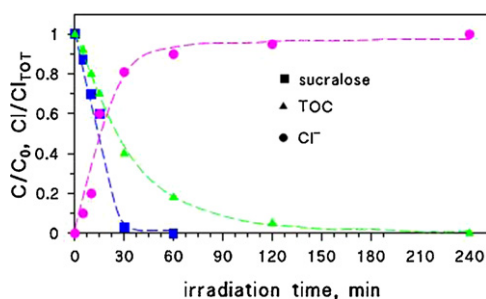


Fig. 5. Degradation of sucralose 15 mg/L, TOC disappearance and chloride evolution as a function of irradiation time in the presence of TiO<sub>2</sub> (200 mg/L).

Total organic carbon measurements were carried out on samples subjected to heterogeneous photocatalysis, to assess sucralose mineralization. Comparing the disappearance profile of sucralose with the organic carbon curve (TOC), we noted that mineralization occurs fast. The TOC curve is only lightly delayed, in agreement with the limited TPs formation evidenced above. Total organic carbon was halved after 30 min of irradiation; a rapid kinetics up to 2 h of irradiation permits a transformation to inorganic carbon in excess of 90%. After 4 h of irradiation, complete mineralization is achieved. This trend is consistent with the simultaneous transformation of chlorine atoms into chloride ions: initially, the process rapidly occurred in the first hour of irradiation, reaching up to a release of 80%, while the stoichiometric release was achieved after 4 h of irradiation.

### 3.5. Toxicity evaluation

The toxicity of irradiated samples was evaluated by monitoring changes in the natural emission of the luminescent bacteria *V. fischeri* when exposed to toxic compounds. Several aqueous samples subjected to heterogeneous photocatalytic process (TiO<sub>2</sub>) at different irradiation times were analyzed to estimate the percentage of inhibition of each sample. The data are collected in Fig. 6. The initial sucralose solution (0 min of irradiation–distilled water) exhibits an inhibition of 5%. The toxicity profile shows a rapid increase of the inhibition percentage in the early steps of the photocatalytic process, reaching 23% just after 10 min of irradiation. The measured inhibition has to be attributed to the formation of toxic intermediates. It is worth mentioning that the highest toxicity observed is in

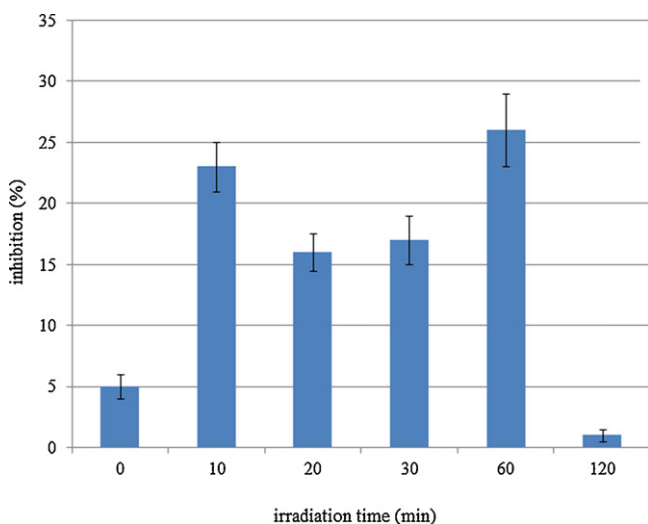


Fig. 6. Inhibition (%) of the luminescence of bacteria *Vibrio fischeri* as a function of the photocatalytic treatment time.

agreement with the maximum concentration of the intermediates formed (see Fig. 4). Although a correlation can be seen between intermediates and toxicity, it was not possible to assess which molecule is responsible for the toxicity. Moreover, the increase of toxicity is moderate and could be affected by experimental uncertainty. From 15–60 min of irradiation the inhibition % still remained higher compared to sucralose initial toxicity. These observations clearly demonstrate that during the photocatalytic treatment, in the period 10–60 min, compounds more toxic than sucralose are formed. After 60 min the toxicity decreased, reaching a value of 1% after 120 min of irradiation. This finding highlights the efficiency of the photocatalytic process in the detoxification of the irradiated solution.

## 4. Conclusions

Results of the present study clearly point out that both heterogeneous TiO<sub>2</sub>, as well as, homogeneous photo-Fenton photocatalytic treatments, are suitable for the elimination of sucralose from the aqueous phase. Design of experiments (DoE) and response surface methodology (RSM) has been shown to be a powerful statistical tool in order to seek the optimal conditions for both AOPs. The conversion of sucralose depends on the operating conditions employed. Optimized operating conditions were: TiO<sub>2</sub> concentration 294 mg/L, light intensity, 698 W/m<sup>2</sup>, for heterogeneous photocatalysis, and Fe<sup>II</sup>, H<sub>2</sub>O<sub>2</sub> concentrations, 6 mg/L and 6 mmol L<sup>-1</sup>, respectively, solution pH=3 for photo-Fenton treatment.

Sucralose was easily degraded under both photocatalytic and photo-Fenton treatments and transformed into few species. These compounds were identified by means of HRMS and a tentative reaction pathway was proposed. Photo-Fenton process chiefly promotes the formation of oxidized products and at a minor extent the cleavage of glycoside bond. Conversely, TiO<sub>2</sub> mediated transformation proceeds through four parallel pathways, where also hydroxylation and dechlorination reactions are significant. Time profiles observed for TPs production strengthens the assumptions made about structures and mechanism of sucralose transformation.

## Appendix A. Supplementary data

Supplementary data associated with this article can be found, in the online version, at <http://dx.doi.org/10.1016/j.apcatb.2012.08.043>.

## References

- [1] J.F. Kenny, N.L. Barber, S.S. Hutson, K.S. Linsey, J.K. Lovelace, M.A. Maupin, U.S. Geological Survey Circular 1344, USGS, 2009, 52p.
- [2] R. Loos, B.M. Gawlik, K. Boettcher, G. Locoro, S. Contini, G. Bidoglio, *Journal of Chromatography A* 1216 (2009) 1126–1131.
- [3] A. Roberts, A.G. Renwick, J. Sims, D.J. Snodin, *Food and Chemical Toxicology* 38 (2000) 31–41.
- [4] J.W. Kille, J.M. Tesh, P.A. McAnulty, F.W. Ross, C.R. Willoughby, G.P. Bailey, O.K. Wilby, S.A. Tesh, *Food and Chemical Toxicology* 38 (2000) S43–S52.
- [5] M.B. Abou-Donia, E.M. El-Masry, A.A. Abdel-Rahman, R.E. McLendon, S.S. Schiffman, *Journal of Toxicology and Environmental Health, Part A* 71 (21) (2008) 1415–1429.
- [6] S.D. Richardson, *Analytical Chemistry* 82 (2010) 4742–4774.
- [7] R.N. Mead, J.B. Morgan, G.B. Avery Jr., R.J. Kieber, A.M. Kirk, S.A. Skrabal, J.D. Willey, *Marine Chemistry* 116 (2009) 13–17.
- [8] J.P. Finn, G.H. Lord, *Food and Chemical Toxicology* 38 (Suppl. 2) (2000) 7–17.
- [9] H.C. Grice, L.A. Goldsmith, *Food and Chemical Toxicology* 38 (Suppl. 2) (2000) S1–S6.
- [10] G.G. Briggs, *Journal of Agricultural and Food Chemistry* 29 (1981) 1050–1059.
- [11] C. Minero, D. Vione, *Applied Catalysis B: Environmental* 67 (2006) 257–269.
- [12] C. Minero, *Catalysis Today* 54 (1999) 205–216.
- [13] A.V. Emeline, V.K. Ryabchuk, N. Serpone, *Journal of Physical Chemistry B* 109 (2005) 18515–18521.
- [14] M. Khajeh, *Journal of Supercritical Fluids* 55 (2011) 944.

- [15] M. Tamimi, S. Qourzal, N. Barka, A. Assabbane, Y. Ait-Ichou, *Separation and Purification Technology* 61 (2008) 103–108.
- [16] H. Katsumata, S. Kaneco, T. Suzuki, K. Ohta, Y. Yobiko, *Chemical Engineering Journal* 108 (2005) 269–276.
- [17] A.N. Módenes, F.R. Espinoza-Quiñones, D.R. Manenti, F.H. Borba, S.M. Palácio, A. Colombo, *Journal of Environment Management* 104 (2012) 1–8.
- [18] I. Michael, E. Hapeshi, C. Michael, D. Fatta-Kassinos, *Water Research* 44 (2010) 5450–5462.
- [19] J.M. Herrmann, *Catalysis Today* 53 (1999) 115–129.
- [20] B. Ohtani, *Advances in Inorganic Chemistry* 63 (2011) 395–430.
- [21] U. Stafford, K.A. Gray, P.V. Kamat, *Heterogeneous Chemistry Reviews* 3 (1996) 77–104.
- [22] Z. Ai, P. Yang, X. Lu, *Journal of Hazardous Materials* 124 (2005) 147–152.
- [23] D. Bahnemann, J. Cunningham, M.A. Fox, E. Pelizzetti, P. Pichat, N. Serpone, in: G.R. Helz, R.G. Zepp, D.G. Grosby (Eds.), *Aquatic and Surface Photochemistry*, Lewis Publishers, USA, 1994, pp. 261–316.
- [24] H-H. Huang, D-H. Tseng, L.-C. Juang, *Journal of Hazardous Materials* 156 (2008) 186–193.
- [25] I. Ferrer, E.M. Thurman, *Journal of Chromatography A* 1217 (2010) 4127–4134.